01 Jul 1999

Two-Phase Flow Distribution in 2D Trickle-Bed Reactors

Y. Jiang

M. R. Khadilkar

M. (Muthanna) H. Al-Dahhan
Missouri University of Science and Technology, aldahhanm@mst.edu

M. P. Dudukovic

Recommended Citation

Y. Jiang et al., "Two-Phase Flow Distribution in 2D Trickle-Bed Reactors," *Chemical Engineering Science*, vol. 54, no. 13 thru 14, pp. 2409 - 2419, Elsevier, Jul 1999.
The definitive version is available at https://doi.org/10.1016/S0009-2509(98)00360-1

PERGAMON

Chemical Engineering Science 54 (1999) 2409–2419

Chemical
Engineering Science

Two-phase flow distribution in 2D trickle-bed reactors

Y. Jiang, M.R. Khadilkar, M.H. Al-Dahhan*, M.P. Dudukovic

Chemical Reaction Engineering Laboratory (CREL), Department of Chemical Engineering, Campus Box 1198, Washington University, St. Louis, MO 63130, USA

Abstract

An extended discrete cell model (DCM), based on minimization of energy dissipation rate, is applied to predict two-phase flow distribution in the two-dimensional trickle-bed reactors. The main advantages of DCM are that it can qualitatively capture the experimental observations, and readily distinguish between flow distribution in prewetted and non-prewetted beds, as well as reflect the effects of bed structure and inlet liquid distributor on two phase flow distribution. For comparison purpose, the results of liquid distribution obtained by DCM are compared with both computational fluid dynamics (CFD) simulations and experimental observations in a 2D bed. The achieved qualitative and quantitative agreement justifies the use of DCM in predicting two phase flow distribution in packed beds. A particle wetting factor (f) has been introduced into DCM to account for the influence of particle surface wetting on liquid flow distribution. Analysis of DCM simulations presented based on maldistribution factor (mf) provides a convenient way of quantifying the effects of particle surface wetting, distributor design and bed depth on the two-phase flow field.

Keywords: Two-phase flow distribution; Trickle-bed reactor; Discrete cell model; Flow visualization; Minimization of energy dissipation rate; CFD

1. Introduction

Trickle-bed reactors with gas–liquid cocurrent downflow have been widely used in hydrogenation, hydrodesulfurization and other hydrotreating processes. One of the major challenges in the design and operation of this type of reactor is the prevention of liquid flow maldistribution which causes portions of the bed to be incompletely wetted by the flowing liquid. This results in an underutilized catalyst bed and, hence, reduces reactor performance and productivity, particularly for liquid limited reactions at low liquid mass velocities. Consequently, conventional reactor models that assume a uniform wetting efficiency throughout the reactor are found to over-predict the reaction rate (Funk et al., 1990). The solution to this problem requires a quantitative understanding of flow maldistribution at different scales in trickle beds.

A number of models of the liquid distribution have been developed in the past two decades based on different concepts or governing principles (Herskowitz et al., 1979; Crine et al., 1979; Stanek et al., 1981; Zimmerman and Ng, 1986; Ahtchi-Ali and Pedersen, 1986; Fox, 1987; Melli and Scriven, 1991). Although these efforts have provided insights into liquid flow distribution at a certain level, these models cannot simulate a number of experimental observations. For example, they cannot account for prewetting of the bed, which is known to have a marked influence on liquid flow distribution (Lutran et al., 1991; Ravindra et al., 1997). Thus, there is a need to incorporate such parameters to an engineering model that can reflect these experimental observations in the model predictions.

The objective of this study is to develop a phenomenological, user friendly, model for prediction of liquid and gas flow distribution in trickle-bed reactors. The developed model should be able to capture the experimental observations, and have enough engineering accuracy. Since the trickle bed is treated as a number of inter-connected cells, in this study the flow distribution model developed is called 'discrete cell model' (DCM). The gas and liquid distribution is assumed to be governed by the minimization of total energy dissipation rate in DCM (Holub, 1990). The motivation for this study was

* Corresponding Author. Tel.: 001-314-935-7187; fax: 001-314-935-4832; e-mail: muthanna@wuche.wustl.edu.

0009-2509/99/$ – see front matter
PII: S0009-2509(98)00360-1

provided by the fact that minimization of total energy dissipation rate has been used frequently in engineering models, yet the results from such an approach were always accepted with a degree of scepticism as not being based on fundamentals. In this study, our goal is also to compare the results obtained from the minimization of total energy dissipation rate (DCM) to those that arise from solution of more fundamental momentum and mass balance formulations, i.e. Computational Fluid Dynamics (CFD). However, the intent of this study is not to replace CFD by DCM, but to examine whether an alternative to CFD of engineering accuracy exists in flow modeling in trickle beds and can be used in more convenient in some cases.

Before presenting the strategy involved in the DCM development, and discussing the superiority of DCM to other models, it is necessary to summarize the liquid distribution models in the literature with references to the spatial scales and their governing principles.

1.1. Spatial scales in trickle beds

Since different spatial scales exist in a packed bed (i.e., bed scale, cell scale, particle scale), there is no question that a flow distribution model based on different spatial scales will require computation at different levels. At one extreme, time-consuming computations required to determine liquid flow on the particle-scale (Zimmerman and Ng, 1986), limit the application of this model to small size bed, although this model can reflect partial catalyst wetting on the particle scale. On the other hand, a bed-scale model, which divides the bed into several regions (i.e., central region and wall region, etc.), is too simplistic to capture the important features of the flow field. Therefore, Holub (1990) assumed that a packed bed could be represented as a number of interconnected cells. Each cell consists of a few particles, and each cell has uniform structure and physical properties. The cell size has to be small compared to the bed scale (i.e., bed diameter), to obtain the desired resolution of bed properties and phase distribution, but large compared to the particle scale (i.e., particle diameter), to apply existing phenomenological hydrodynamic models developed in lab-scale packed beds (i.e., two-phase Ergun equations, Holub et al., 1992, 1993). The appropriate cell dimensions to satisfy these criteria were discussed by Vortmeyer (1984). For the exact situation considered in this study, a minimum linear dimension of three particle diameters for each cell has been recommended (Holub, 1990). Fig. 1 represents a typical two-dimensional cell with the velocity convention and coordinate system used in DCM formulations. The nature of such a discrete cell model allows us to obtain flow distribution information (at few particles scale) with reasonable computational efforts.

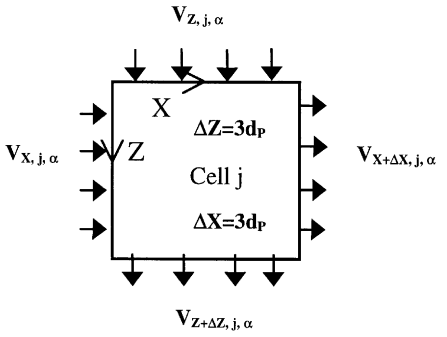

Fig. 1. The coordinate system and velocity conventions for the α phase in the jth cell.

1.2. Governing principles for flow distribution

Because of the complexity of two-phase flow modeling in trickle-bed reactors, different governing principles for flow distribution models have been assumed in the literature. The 'diffusion model' assumed that the irrigation flux satisfies the diffusion equation, which could be solved for a variety of inlet flow distributions (Stanek et al., 1981; Stanek, 1994). This model was not capable of predicting phase separation phenomena that occur in trickle beds. The 'percolation approach' has been used by many researchers to model the flow in trickle beds (Crine et al., 1979; Melli et al., 1991). The model assumed the flow distribution in the bed to be a stochastic process. The liquid was distributed on the network by randomly choosing the bonds in the structure that have flowing liquid. While the model had the merit of representing the liquid structure as discontinuous in the bed, the predictive ability is questionable for the small size of particles since a direct relationship does not exist between the network and bed structure. In a computer-generated packed bed of equally sized spheres, the 'sphere-pack model' predicts the liquid distribution based on developed wetting criteria (Zimmerman and Ng, 1986). The model was able to predict liquid coring, but gas flow was not included in the model. The model was also limited to the case of initially dry spherical particle surface, hence, the effect of particle prewetting could not be accounted for. In the 'discrete cells model' (DCM) (Holub, 1990) addressed in this study, it was assumed that the flow can be determined by the minimum rate of total energy dissipation in the packed bed (i.e. *flow follows the path of the least resistance*). The known porosity variation in the bed could readily be incorporated into DCM by inputting cell porosity values. The type of liquid and gas distributors (i.e. point source; uniform source; irregular source for two fluids) is accounted for by setting two-phase velocity values at inlet cell boundaries. To consider the effect of particle wetting state on the liquid distribution (i.e. prewetted bed and nonprewetted bed), which has been observed by experimental studies (Lutran et al.,

1991; Ravindra et al., 1997), the contribution of capillary pressure has been incorporated into the original DCM, and reported as an extended DCM in this paper.

The superiority of the extended DCM to other flow distribution models can be attributed to its ability to consider (i) effect of bed structure nonuniformity (two-dimensional porosity variations; internals in packed bed); (ii) effects of gas and liquid distributors; (iii) effect of particle prewetting.

2. Extended discrete cell model

Discrete cell model (DCM) was originally formulated by Holub (1990). The fully analysis and detailed implementation of individual aspects of DCM for single-phase modeling (gas flow or liquid upflow) have been recently reported (Jiang et al., 1998). In this paper, DCM is applied to two-phase flow modeling in trickle beds. Since the detail formulation is available elsewhere (Holub, 1990; Jiang et al., 1998), only the key model equations and extended parts pertinent to two phase flow are presented here.

The equation for the macroscopic mechanical energy balance for phase α in the jth unit cell can be expressed in continuum form by Eq. (1), and is based on the following key assumptions: (i) Each unit cell of the bed has a uniform porosity (ε_j, which can vary from cell to cell), and constant phase holdup as well as constant phase properties; (ii) Steady-state flow distribution is considered in the entire bed and fluids are incompressible; (iii) No phase change occurs at the gas–liquid interface. Contribution of chemical reaction to the flow distribution is not accounted for in this model.

$$\sum_{i=1}^{4}\left\{\frac{1}{2}\left(\rho\left(\frac{V}{\varepsilon}\right)^2\cdot\left(\frac{V}{\varepsilon}\right)\right)_\alpha s_i + P\left(\frac{V}{\varepsilon}\right)_\alpha s_i + \hat{\Phi}\left(\rho\left(\frac{V}{\varepsilon}\right)\right)_\alpha s_i\right\}_{j,\text{in}} - \sum_{i=1}^{4}\left\{\frac{1}{2}\left(\rho\left(\frac{V}{\varepsilon}\right)^2\cdot\left(\frac{V}{\varepsilon}\right)\right)_\alpha s_i + P\left(\frac{V}{\varepsilon}\right)_\alpha s_i + \hat{\Phi}\left(\rho\left(\frac{V}{\varepsilon}\right)\right)_\alpha s_i\right\}_{j,\text{out}} - \left(\frac{E}{\varepsilon}\right)_{V,j,\alpha} = 0. \tag{1}$$

For a 2D rectangular cell (j) as depicted in Fig. 1, the mechanical energy dissipation rate of phase α, $E_{V,j,\alpha}$, can be written in the discretized form as follows:

$$E_{V,j,\alpha} = \frac{\rho_\alpha}{2}\left\{\frac{1}{\varepsilon_{j,\alpha}^2}(V_X^3 S_X - V_{X+\Delta X}^3 S_{X+\Delta X})_{j,\alpha} + \frac{\rho_\alpha}{\varepsilon_{j,\alpha}^2}(V_Z^3 S_Z - V_{Z+\Delta Z}^3 S_{Z+\Delta Z}^3)_{j,\alpha} + \left(\frac{1}{\varepsilon_{j,\alpha}}\right)^3[(a_{j,\alpha}+b_j|V_{X,j,\alpha}|)V_{X,j,\alpha}^2 + (a_{j,\alpha}+b_j|V_{X+\Delta X,j,\alpha}|)V_{X+\Delta X,j,\alpha}^2](\text{Vol})_j + \left(\frac{1}{\varepsilon_{j,\alpha}}\right)^3[(a_{j,\alpha}+b_j|V_{Z,j,\alpha}|)V_{Z,j,\alpha}^2 + (a_{j,\alpha}+b_j|V_{Z+\Delta Z,j,\alpha}|)V_{Z+\Delta Z,j,\alpha}^2](\text{Vol})_j - [g_X(V_X+V_{X+\Delta X})_{j,\alpha}\cos^2\gamma_X + g_Z^2(V_Z+V_{Z+\Delta Z})_{j,\alpha}\cos^2\gamma_Z](\text{Vol})_j\right\}. \tag{2}$$

A discretized form of the macroscopic mass balance equation can be similarly written as

$$(\rho V_X S_X - \rho V_{X+\Delta X}S_{X+\Delta X})_{j,\alpha} + (\rho V_Z S_Z - \rho V_{Z+\Delta Z}S_{Z+\Delta Z})_{j,\alpha} = 0. \tag{3}$$

A detaied derivation of each term in Eq. (2) is available in Holub (1990). The complete model of flow distribution is to determine the two-phase velocities at each cell interface by minimization of the total energy dissipation rate over the entire bed domain. It is essentially a nonlinear, multivariable minimization problem as given in Eq. (4) subject to the mass balance constraint [Eq. (3)] for each phase in cell j, and additional constraints to reflect gas and liquid velocities at the bed inlet and at other boundaries of the bed (i.e., *phase velocities in the cell adjacent to the wall are zero in the direction normal to the wall*).

$$\text{Minimize:} \qquad E_{V,\text{bed}} = \sum_{\alpha=1}^{2}\sum_{j=1}^{N} E_{V,j,\alpha}. \tag{4}$$

The subroutine DN0ONF from the International Mathematical Statistics Library (IMSL) was used to solve this nonlinear multivariable minimization problem.

To get phase velocities from the above equations, we have to solve for cell phase holdup ($\varepsilon_{j,\alpha}$) corresponding to a set of assumed phase velocities. It can be done by equating cell pressure drops in the gas and liquid phase (in absence of capillary pressure).

$$\left(\frac{\Delta P_{G,j}}{\Delta L}\right) = \left(\frac{\Delta P_{L,j}}{\Delta L}\right). \tag{5a}$$

Then pressure drops are expressed in terms of dimensionless pressure drop functions ($\psi_{G,j}$ for gas, $\psi_{L,j}$ for liquid).

$$\frac{\Delta P_{G,j}}{\Delta L} = \rho_G g(\Psi_{G,j} - 1), \tag{5b}$$

$$\frac{\Delta P_{L,j}}{\Delta L} = \rho_L g(\Psi_{L,j} - 1). \tag{5c}$$

Substitution of Eqs. (5b) and (5c) into Eq. (5a) yields Eq. (6)

$$\Psi_{L,j} = 1 + \frac{\rho_G}{\rho_L}(\Psi_{G,j} - 1). \tag{6}$$

To correlate these pressure drop functions to cell flow velocities, two-phase flow Ergun equations (Holub et al., 1992, 1993) as given in Eq. (6a) and (6b) are used. This is equivalent to utilizing the concept of relative permeability discussed by Saez and Carbonell (1985).

$$\Psi_{G,j} = \left(\frac{\varepsilon_j}{\varepsilon_j - \varepsilon_{L,j}}\right)^3 \left[\frac{E_1 Re_{G,j}}{Ga_{G,j}} + \frac{E_2 Re_{G,j}^2}{Ga_{G,j}}\right], \tag{6a}$$

$$\Psi_{L,j} = \left(\frac{\varepsilon_j}{\varepsilon_{L,j}}\right)^3 \left[\frac{E_1 Re_{L,j}}{Ga_{L,j}} + \frac{E_2 Re_{L,j}^2}{Ga_{L,j}}\right]. \tag{6b}$$

Thus, substitution of $\psi_{G,j}$ and $\psi_{L,j}$ [from Eq. (6a) and (6b)] into Eq. (6) yields a nonlinear equation in terms of phase holdups ($\varepsilon_{j,\alpha}$) and cell-phase velocities which can be readily solved if flow velocities are known.

The essential part of extended DCM is the treatment of the drag force by taking into account capillary pressure. The pressure difference in the gas and liquid phase could be correlated with the capillary pressure (Grosser et al., 1988) and a particle wetting factor, f, as

$$P_{G,j} - P_{L,j} = P_{C,j}(1 - f), \tag{7}$$

where the capillary pressure, $P_{c,j}$, in packed bed can be written as Eq. (8) in terms of the well-known Leverett's J-function (Leverett, 1941) as suggested by Grosser et al. (1988).

$$P_{C,j} = \frac{(1 - \varepsilon_j)}{\varepsilon_j d_P} E_1^{0.5} \sigma J(s_{W,j}). \tag{8}$$

When complete particle wetting occurs ($f = 1$) the pressure difference between the gas and liquid phase disappears. This is the case treated in the original DCM (Holub, 1990). The pressure difference would reach a maximum (equal to the capillary pressure, $P_{c,j}$) when the factor f is equal to zero (completely non-prewetted case). Depending on the nature of the particle surface and liquid–solid contact angle, the value of the factor f is somewhere in the range of zero to one.

Thus, phase holdup is solved for by equating the difference of pressure drops in gas and liquid phases to the capillary pressure times the factor $(1 - f)$ as given in Eq. (9).

$$\frac{\Delta P_{G,j}}{\Delta L} = \frac{\Delta P_{L,j}}{\Delta L} + \frac{(1 - \varepsilon_j)}{\varepsilon_j d_P} E_1^{0.5} \sigma (1 - f) \frac{\Delta J(s_{W,j})}{\Delta L}. \tag{9}$$

Similarly to Eq. (6), we can get Eq. (10) in terms of dimensionless pressure drop functions, and from it we can solve for liquid holdup.

$$\Psi_{L,j} = 1 + \frac{\rho_G}{\rho_L}[\Psi_{G,j} - 1] + \frac{(1 - \varepsilon_j)}{\rho_L \varepsilon_j d_P} E_1^{0.5} \sigma (1 - f) \left[\frac{b}{s_{W,j}(1 - s_{W,j})}\right] \times \frac{\Delta J(s_{W,j})}{\Delta L}, \tag{10}$$

when $\psi_{G,j}$ and $\psi_{L,j}$ are obtained from Eq. (6a) and (6b) as before.

Before presenting and justifying the modeling results of DCM, it is desired to summarize the experimental observations of the liquid distribution to get basic ideas about what the liquid distribution looks like in trickle-bed reactors.

3. Experimetal observations

The limited availability of experimental data on flow distribution, without the interfering effects of the measurement, causes uncertainty in validation of flow distribution models. The most prominent method of determining phase distribution in trickle beds has been to collect the liquid and gas at the outlet of the bed (Herskowitz and Smith, 1979). While care has been taken to minimize the disturbances to the flow pattern, it is still expected that flow redistribution occurs in the exit region. Recently non-intrusive tomographic techniques (Chaouki et al., 1997) for phase distribution imaging have shown some promises of obtaining a much more complex flow pattern in trickle beds (Lutran, et al., 1991; Kantzas, 1994; Toye et al., 1994). Lutran et al. (1991) visualized liquid distribution in a rectangular trickle bed using a medical computed tomography (CT) scanner with a quiescent gaseous phase and non-porous spherical particles. A series of visualization experiments were qualitatively presented in which flow patterns were recorded as a function of liquid flow rate, particle size, liquid inlet configuration, surface tension and flow history. It was clearly shown that the effect of particle pre-wetting on the liquid flow pattern is dominate. A quantitative measurement of liquid holdup was reported in Kantzas' work (1994) by using commercial X-ray CT scanner. X-ray tomography was also used by Toye et al. (1994) for imaging the gas–liquid–solid distribution in trickling filters. The bed scanned has a diameter of 0.6 m and a height of 2 m with particle element of 4.4 cm.

Although CT technique can provide quantitative information of phase fraction distribution in trickle beds, not enough experimental data is reported in the open literature. In particular, no detailed data about the porosity distribution were reported in the literature. This makes the quantitative verification of the flow model by experimental data difficult to achieve. Others explored to use the simple approach to get direct visualizations of the liquid flow in packed beds. For example, Ravindra et al. (1997) recently presented direct insights in the liquid flow distribution in the prewetted and non-prewetted 3D rectangular bed by dye adsorption method. It was shown again that the effect of prewetting on liquid distribution is significant. To confirm this observation in the pseudo-2D packed bed, an exact replica of the '2D' model packed-bed was constructed out of transparent materials

in this study. PC-based CCD (charge couple device) image technique (CCD video camera, computer image software, etc) is used to obtain direct visualization of the liquid flow. It allows us to have porosity information on which DCM simulations have to be based.

Working fluids used in the experiments are air and colored water (black). Figs. 2a and b confirm the effect of particle prewetting at a liquid superficial mass velocity of 3.52 kg/m^2 s in 2D bed. It is apparent that a liquid filament pattern was observed in the case of the non-prewetted packing whereas liquid film flow occurs in the prewetted bed.

4. Modeling results and discussion

The modeling results are presented for a '2D' rectangular bed, 7.2 cm (width) $\times$ 28.8 cm (height) $\times$ 0.9 cm (thickness), referred henceforth as '*model bed*', which has an average bed porosity of 0.415 corresponding to the value measured experimentally. To examine the cell porosity effect on flow distribution, the internal porosity profiles were specially designed by using a pseudo- 'random' porosity distribution generated by computer program with given constraints (i.e. porosity is kept in the range of 0.36–0.44 with an average of 0.406 for the inner bed region away from the walls while higher porosity of 0.44 is assigned to the wall region) (see Fig. 3a). Two transverse locations with low average porosity were deliberately designed as plotted in Fig. 3b. This bed is divided into eight cells in width (n_C) and 32 cells in length (n_R) and is 1 cell thick (n_T). Each cell has a size of $3d_p \times 3d_p \times 3d_p$ (0.9 cm $\times$ 0.9 cm $\times$ 0.9 cm) as depicted in Fig. 1. The bed walls are considered to be impermeable boundaries. The liquid inlet distribution was assigned as uniform, single point source and as two points source to indicate different liquid distributors. The inlet distribution for the gas phase was assigned as uniform in all the case studies.

To quantify the liquid flow maldistribution, it is of interest to compare the deviation from uniform velocity profiles in term of the liquid maldistribution factor, mf, defined as

$$\mathrm{mf} = \sqrt{\sum_{i=1}^{r} \frac{A_i}{A_0}\left(1 - \frac{|V_i|}{V_0}\right)^2}, \tag{11}$$

When the liquid flow distribution is uniform over the bed cross section, mf is equal to zero and mf increases as the distribution becomes less uniform. The effect of the parameters (i.e. particle prewetting, liquid distributor, particle size) on flow distribution can be quantitatively described by the value of mf. The axial mf profile reflects the effect of bed depth on the flow distribution. Since higher liquid velocity corresponds to the higher liquid holdup, the trend of mf is essentially similar to the liquid holdup trend in whole bed domain.

4.1. Comparison of DCM and CFD simulations

The main assumption of DCM is that the flow is governed by the minimum rate of total energy dissipation in the bed. The complete theoretical justification for this assumption has been provided for linear relationships between fluxes and driving forces and rests on the principle of entropy maximization (Jaynes, 1980). Recently,

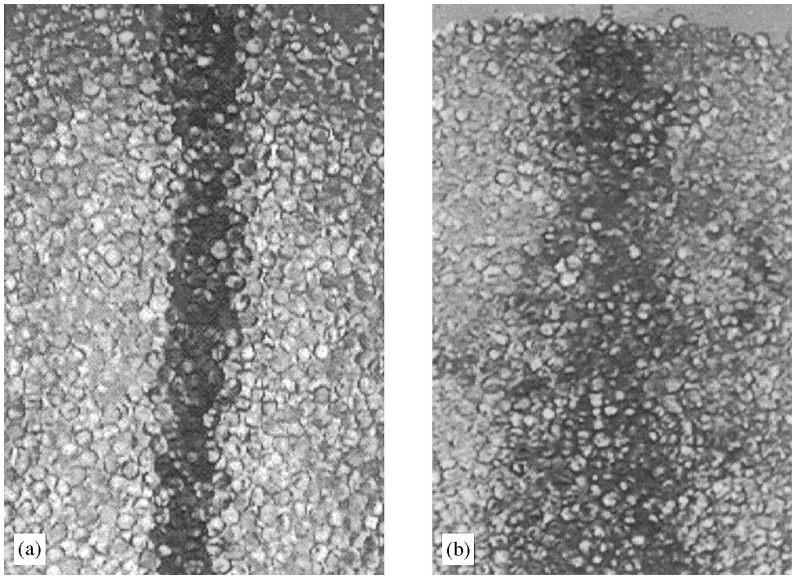

Fig. 2. The CCD images of liquid distribution in '2D' packed beds with single point source liquid inlet ($\bar{U}_L = 0.00352$ m/s; $U_g = 0$ m/s); Glass beads of 3 mm (a) Non-prewetted bed; (b) prewetted bed.

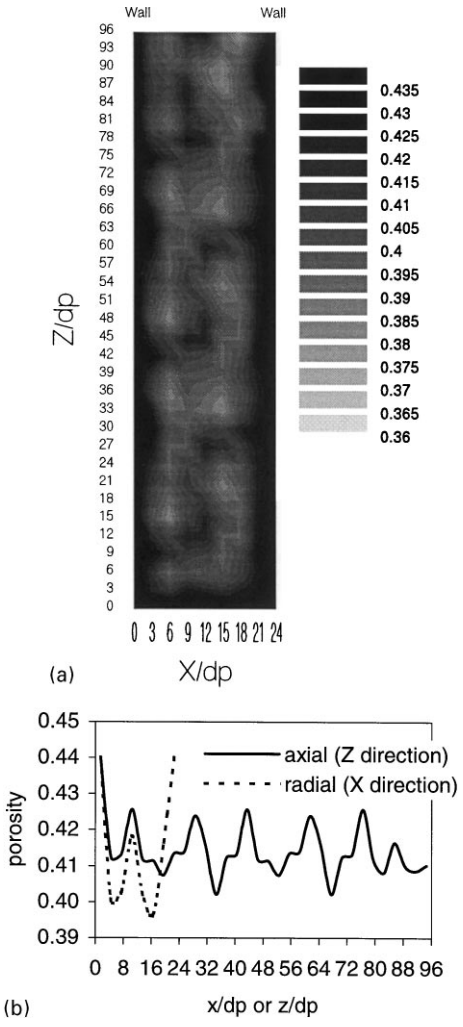

Fig. 3. (a) Local porosity distribution in model bed; Random internal porosity (0.36 ~ 0.44). Higher porosity of 0.44 at the walls. Darker color corresponds to higher porosity. (b) Average porosity profiles in X and Z directions in model bed.

for non-linear systems, particularly non-parallel gas flow or liquid up-flow in the packed beds (*where the local phase holdup is equal to the local porosity*), agreeable numerical comparisons of DCM and CFD (using CFDLIB code as described below) have been achieved (Jiang et al., 1998). The difference between DCM and CFDLIB simulations was found to be always within 10% over a wide range of Reynolds numbers. Nevertheless, it is desired to compare the predictions of these two methods for the gas–liquid two-phase flow system which is of interest in this paper. For this purpose, the Computational Fluid Dynamics code, CFDLIB developed by Los Alamos National Laboratory (Kashiwa et al., 1994), has been used to obtain the results for comparison with the DCM predictions. The governing equations that serve as the basis for the CFDLIB codes and drag closures used in the simulation are given below

Equation of continuity:

$$\frac{\partial \rho_k}{\partial t} + \nabla \rho_k u_k = \langle \rho_k \dot{\alpha_k} \rangle. \quad (12a)$$

(Accumulation) (Convection) (Mass source)

Equation of momentum:

$$\frac{\partial \rho_k u_k}{\partial t} + \nabla \cdot \rho_k u_k u_k = -\nabla \cdot \langle \alpha_k \rho_0 u_k' u_k' \rangle$$

(Accumulation) (Convection) (Reynolds stress)

$$-\theta_k \nabla p + \rho_k g$$

(Mean pressure) (Body force)

$$+ \langle [(p_0 - p) I_0 - \tau_0] \cdot \nabla \dot{\alpha_k} \rangle + \langle \rho_0 u_0 \dot{\alpha_k} \rangle$$

(Exchange term) (Mass source)

$$+ \nabla \cdot \langle \alpha_k \tau_0 \rangle - \nabla \theta_k (p_0 - p) \quad (12b)$$

(Average stress) (Non-equilibrium pressure)

This set of equations is exact with no approximations other than the ensemble averaging used in the two-fluid model approach. The special case of one fixed phase (packed bed) has also been incorporated in the code for single and two-phase flow simulation. Boundary conditions for inflow, outflow, and free/no slip at the reactor walls has been directly specified (Kumar, 1994). The important term in simulating trickle bed is the interphase drag term. The code models the drag force as a product of a user defined exchange coefficient (X_{k1}), phase volume fraction (θ_k, θ_1), and relative velocity of the two phases k and l as given below

$$F_{D(k-l)} = \theta_k \theta_l X_{kl} (u_k - u_l), \quad (13)$$

where the X_{kl} is modeled by the modified Ergun equation (Holub et al., 1992; Saez and Carbonell, 1985) with universal Ergun constants in this study. This drag form is the same as that used in DCM simulation. The drag between flowing phases has been ignored for complete wetted particles. To keep the consistency with the discrete cell approach used in DCM, free-slip boundary conditions are used for the reactor walls in CFD simulation. The spatial discretization of the model bed is also the same in both methods.

For given set of operating conditions (U_l = 0.00148 m/s; U_g = 0.05 m/s; prewetted bed), the predicted relative gas flow superficial velocity profiles by CFD and DCM at different heights (Z/d_p) in the bed are tracking well each other, and similar to the results obtained in the single-phase flow system (Jiang et al., 1998). The comparison of the complete data set in all cells is plotted in Fig. 4. Quantitatively, the agreement between the two model predictions for gas flow is good, and the differences in prediction of gas flow by CFD and DCM are less than 13%.

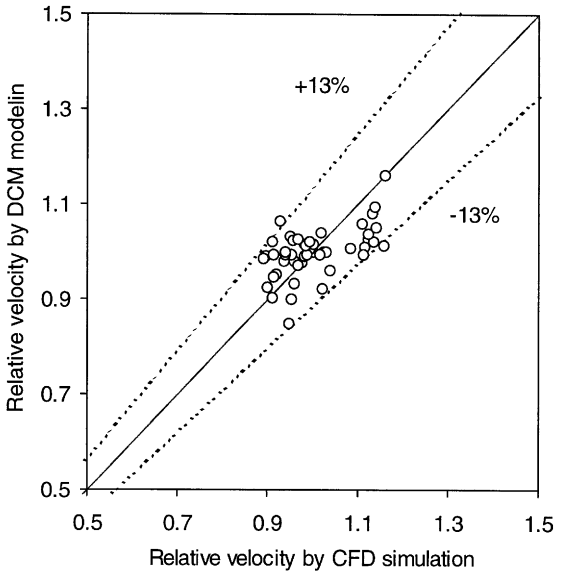

Fig. 4. Comparison of the predicted gas superficial velocities (relative) for all the cells by DCM and CFD. Inlet uniform superficial velocities: $U_l = 0.00148$; $U_g = 0.05$ m/s; Completely prewetted packed bed. (*The relative superficial velocity is defined as the local superficial velocity* (V_j) *divided by the overall superficial velocity* (V_o).

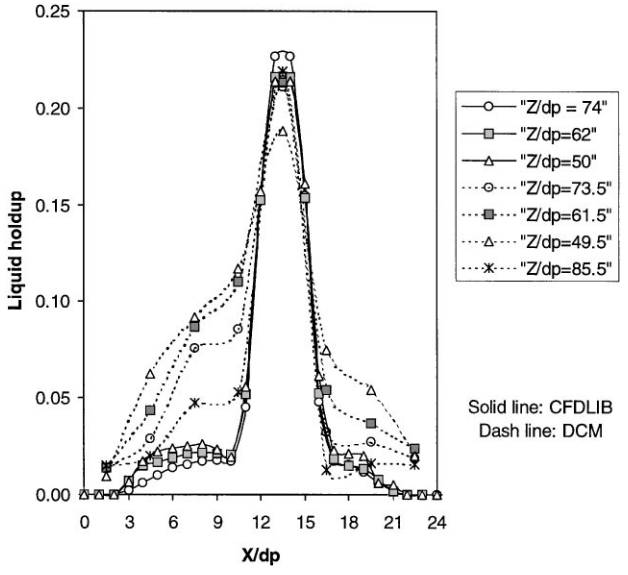

Fig. 5. Comparison of predicted liquid holdup at specific levels by DCM and CFD. $\bar{U}_L = 0.00148$ m/s (U_l (PS$_1$) = 0.01184 m/s); $U_g = 0.05$ m/s; Non-prewetted packing.

The comparison of predicted liquid holdup at the specific levels of bed is shown in Fig. 5 for the case of a single-point source liquid inlet (PS). The comparison of predicted liquid holdup by both methods is reasonable particularly in the central core. The difference in the prediction of liquid holdup by two methods (CFD and DCM) at locations far from the central flow indicates that the DCM seems to be more sensitive to local porosity values than CFD, and give more predicted liquid spreading. These numerical results can be qualitatively compared to experimental observations presented in Fig. 2a, which illustrates that rivulet flow is affected by the local porosity which causes it not to flow straight down through the bed. Extensive numerical comparisons of DCM and CFDLIB under different conditions including no-slip at the wall, and quantitative comparisons of numerical simulations (DCM, CFD) and experimental data are in progress.

4.2. Effect of liquid distributor

Three types of liquid inlet distributors: single point source (PS$_1$), two-points source (PS$_2$) and uniform distributor (UF) have been used to demonstrate the effect of liquid distributors on the liquid distribution in a non-prewetted packed bed. The boundary (inlet) values of the liquid superficial velocities at the top cell layer of the bed were assigned to keep the same volumetric liquid feed rate for all types of liquid distributors studied. With liquid point source inlets, as shown in Fig. 6a for single inlet and Fig. 6b for two inlets, it was found that the number of liquid channels formed in the non-prewetted packed bed corresponded to the number of liquid point sources. This observation is reflected in the result shown in Fig. 2a. With the uniform liquid inlet, as shown in Fig. 6c, however, uniform liquid distribution occurs only in the entrance region, then channel flow forms in the downstream region due to the nonuniform porosity and capillary pressure effect. Under the chosen set operating conditions (in Table 1), an onset of formation of liquid channels (i.e phase segregation) is seen at a depth of 2 cm and formation of distinct channels occurred at a bed depth of 8 cm. These channels meandered, merged, and split as experimentally observed by Ravindra et al. (1997). It can be concluded that liquid channel flow is typical in non-prewetted beds. These DCM results are qualitatively comparable with direct flow visualizations (Figs. 2a and Ravindra et al.'s photo observations, 1997). A comparison of liquid maldistribution factor (mf) along the bed for different distributors is given in Fig. 6d. The effect of liquid distributor on liquid flow maldistribution is significant in the upper half of the bed (in non-prewetted beds) and is less pronounced at depths exceeding 50 particle diameters (15 cm) for total bed length of 96 particle diameters.

4.3. Effect of particle prewetting

Experimental observations have corroborated the fact that the effect of particle prewetting on liquid distribution is significant and causes more liquid spreading in 3D rectangular bed (Lutran et al., 1991; Ravindra et al.,

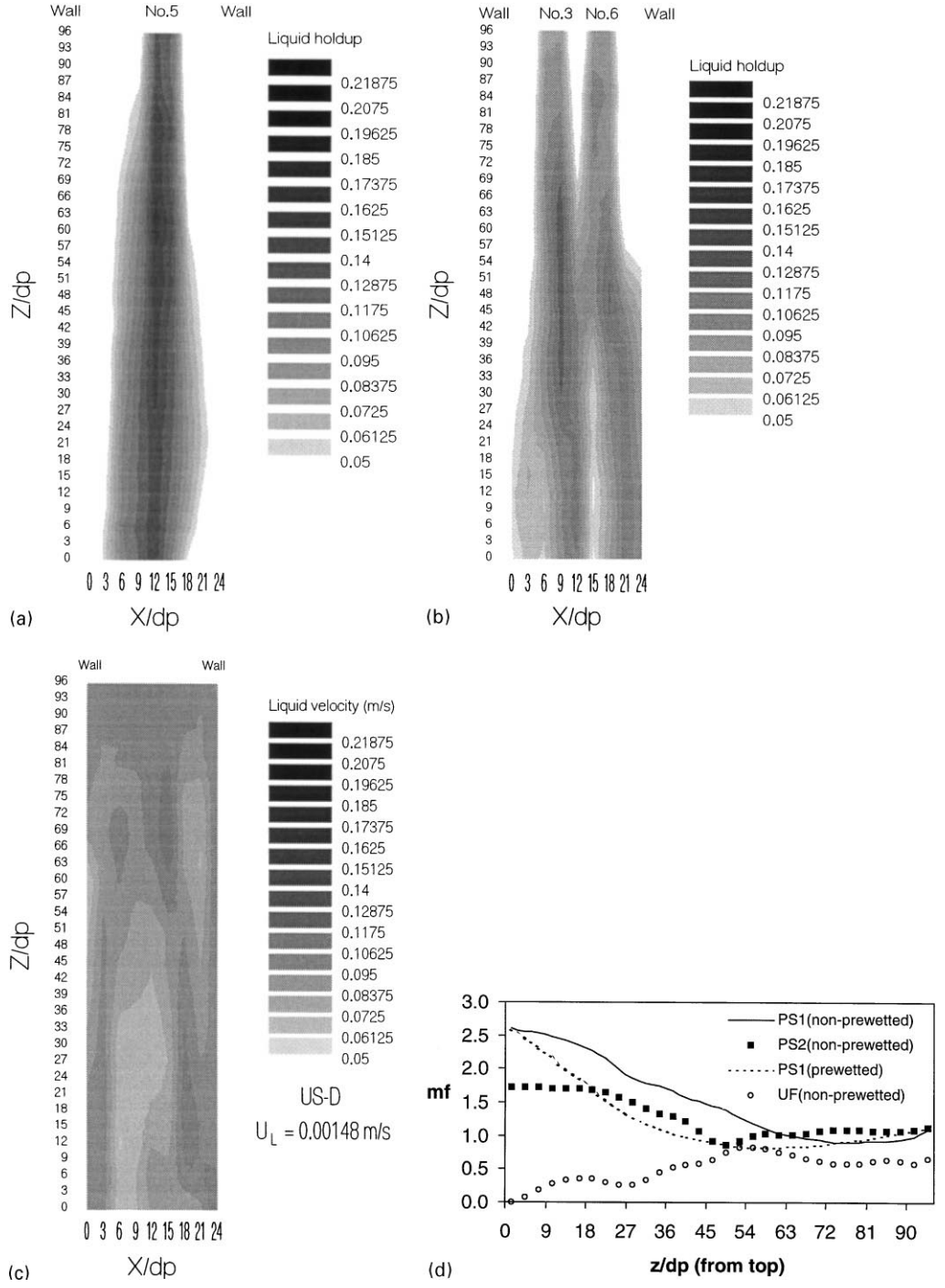

Fig. 6. (a) Liquid holdup distribution with single liquid point source inlet (located at No. 5 cell from left) by DCM. $\bar{U}_L = 0.00148$ m/s (U_l (PS_1) = 0.01184 m/s); $U_g = 0.05$ m/s; Non-prewetted packing. (b) Liquid holdup distribution with two liquid points source inlet (located at No. 3 cell and No. 6 cell from left) by DCM. $U_L = 0.00148$ m/s (U_l (PS_2) = 0.00592 m/s); $U_g = 0.05$ m/s; Non-prewetted packing. (c) Liquid holdup distribution in whole domain of the non-prewetted packed bed with uniform liquid distributor by DCM. $U_l = 0.00148$ m/s; $U_g = 0.05$ m/s. (d) Comparison of liquid flow maldistribution calculated by DCM along the bed for different liquid distributors. $\bar{U}_L = 0.00148$ m/s; $U_g = 0.05$ m/s.

1997). The CCD video images in Figs. 2a and b also confirm the same finding in pseudo-2D bed. It was reported that lower capillary pressure (by lower liquid surface tension, lower contact angle (θ) at the three-phase contact line) caused more particle wetting in the bed, and accordingly, caused an increase in overall liquid holdup (Levec, et al., 1986). In order to predict these experimental observations, we have incorporated a particle surface wetting factor (f) into DCM as described earlier. Fig. 7a shows the liquid holdup distribution in the entire

Table 1
Summary of operating conditions used in flow simulations

$U_l = 0.00148$ m/s $U_g = 0.050$ m/s (superficial velocity)			
Completely prewetted bed		Completely nonprewetted bed	
Gas inlet	Liquid inlet	Gas inlet	Liquid inlet
UF	PS_1, PS_2; UF	UF	PS_1

UF: uniform.
PS_1: single-point source located at top layer* at No. 5 cell.
PS_2: two-points source located at top layer at No. 3 and No. 6 cell.
Note: There are 8 cells on the top layer from No. 1–No.8.

completely prewetted bed with a single-point liquid inlet (PS_1) (*actually one cell inlet*). For further comparison, Figs. 7b and c show the predicted liquid holdup at the specific levels ($Z/d_p = 94.5$; 73.5; 61.5; 49.5 from bottom) in the completely prewetted bed ($f = 1$) and in non-prewetted bed ($f = 0$), respectively. More liquid spreading is obvious in the prewetted bed whereas the effect of capillary pressure on liquid holdup distribution is apparent in the non-prewetted bed. It is the reason for liquid channel flow formation in the non-prewetted bed. If the bed is pre-filled with liquid, thin liquid films will be formed around the particle surfaces, in addition to the pores being filled by liquid, even when the liquid is

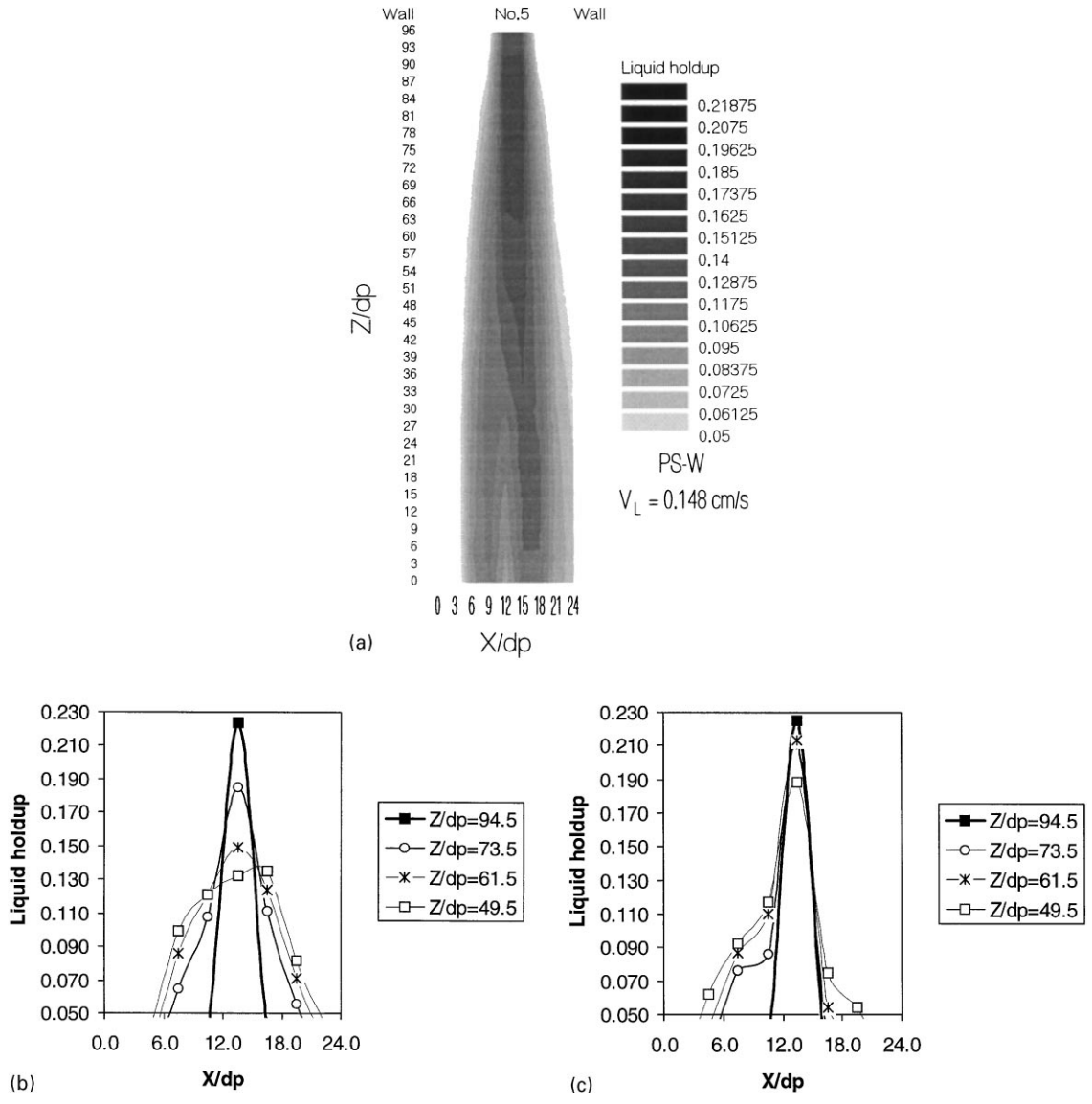

Fig. 7. (a) Liquid holdup distribution in the whole domain of the completely prewetted packed bed ($f = 1$). $\bar{U}_L = 0.00148$ m/s (U_l (PS_1) = 0.01184 m/s); $U_g = 0.05$ m/s; Point liquid distributor (PS_1). (b) Liquid holdup distribution at specific levels (Z/d_p) in the completely prewetted packed bed ($f = 1$), $\bar{U}_L = 0.00148$ m/s (U_l (PS_1) = 0.01184 m/s); $U_g = 0.05$ m/s; Point liquid distributor (PS_1); Overall liquid holdup = 0.0758. (c) Liquid holdup distribution at specific levels (Z/d_p) in the completely non-prewetted packed bed ($f = 0$), $\bar{U}_L = 0.00148$ m/s (U_l (PS_1) = 0.01184 m/s); $U_g = 0.05$ m/s; Point liquid distributor (PS_1); Overall liquid holdup = 0.0716.

drained off. These liquid films nullify the effect of capillary pressure and help spreading of the incoming liquid. Therefore, as expected, more liquid spreading in prewetted bed is observed as shown by DCM simulation in Fig. 7a. The overall liquid holdup in the prewetted bed is 6% higher than in the non-prewetted bed at the same operating conditions (as seen in Figs. 7b and c). It is in agreement with Levec's et al experimental finding (1986).

It is also of interest to consider Fig. 6d, which shows that the liquid flow distribution with one point source liquid inlet in the prewetted bed is better in most portions of the bed (except the inlet region) than that obtained by two points source liquid inlet in the non-prewetted bed. This also corporates evidences of better performance in prewetted bed. The only detrimental consequence of prewetting is liquid 'wall flow' which occurs in the case of the completely prewetted bed with uniform liquid inlet, since liquid spreads more easily until it reaches the wall and then continues along it resulting in the observed wall flow.

Although only two extremes of particle wetting are considered here, the real liquid distribution may occur somewhere between two limiting cases ($f = 0$ and 1.0) depending on the particle surface and fluid properties of system. It is expected that the value of surface wetting factor, f, is associated with three-phase interfacial-phenomena, such as liquid–solid contact angle, liquid surface tension, particle internal porosity, etc. Local liquid vaporization may also cause local particle wetting non-uniformity, and further affect the value of f. It is also believed that the differences between non-porous and porous particles are reflected in different values of f, and further cause different liquid distribution as observed experimentally by Ravindra et al., (1997). One should note that the surface wetting factor (f) used in this paper is not the same as the 'particle external wetting efficiency' which has been widely used in the literature. The particle surface wetting factor, f, is essentially a lumped parameter which reflects the contributions of a number of factors to the two phase flow distribution. Although the experimental measurements of f values are not available so far, the flow simulations based on two limiting values of f (zero and one) essentially cover the range of possible liquid distribution at given operating conditions (see Figs. 6a and 7a), which is valuable in examining possible trickle-bed scale-up and design.

5. Conclusions and final remaks

An extended discrete interconnected cell model (DCM) was developed for simulation of two phase flow in trickle-bed reactors. Due to the nature of DCM, structural nonuniformities and different liquid inlet distributors can be readily incorporated into the model. Particle wetting characteristics are accounted for in the model by introducing the particle wetting factor (f) to distinguish between the flow patterns in prewetted and non-prewetted beds. The model predicted results are quantitatively comparable with those obtained from computational fluid dynamic codes (CFDLIB). Simulated liquid holdup distribution data qualitatively agree with the direct flow visualization experiments, which have not been achieved by other available models. Two bounds (corresponding to the completely prewetted and completely non-prewetted catalyst) on the liquid flow distribution at given operating conditions can be provided by DCM model. The effect of liquid distributor on liquid flow distribution is significant in the upper half of the bed. Both extensive numerical comparison of DCM and CFD, and quantitative comparison of numerical simulation and experiment data are in progress to further verify this new model. In regard of the computational efficiency of DCM, which is essentially formulated as a non-linear multi-variable optimization problem, more effective optimization algorithms are desired for industrial scale problems with a large number of cells (as compared with only 256 cells used in this study).

The advantage of DCM will become more apparent when we utilize it to compute not only just flow distribution but also reactor performance since problem formulation in DCM is easier compared to CFD. At this point, we re-emphasize that DCM is not suggested as a replacement for CFD. However, it is shown here that when one is interested only in the coarse structure of the flow pattern, DCM can provide answers comparable to those obtained by CFD.

Acknowledgements

The authors acknowledge the financial support of the industrial sponsors of the Chemical Reaction Engineering Laboratory (CREL) and Dr. R. A. Holub for providing the original version of the DCM code.

Notation

a	constant in Leverett's function (= 0.48 for air–water system)
a_j,	working variable $[E_1(1-\varepsilon_j)^2\mu_\alpha/(\rho_\alpha\varepsilon_j^3 d_p^2)]$
b	constant in Leverett's function (= 0.036 for air–water system)
b_j	working variable $[E_2(1-\varepsilon_j)/(\varepsilon_j^3 d_p)]$
d_p	particle diameter, (0.003 m)
E_1, E_2	Ergun equation constants ($E_1 = 150$; $E_2 = 1.75$)
$E_{v,j,\alpha}$	energy dissipation rate of phase α in the jth cell, J/s (based on $V_{j,\alpha}$)
$E_{v,\mathrm{bed}}$	total energy dissipation rate in the bed, J/s
f	particle wetting factor

g_i, $i = x,z$	gravitational acceleration in the i direction, ($g_x = 0$; $g_z = 9.8$ m/s^2)
$Ga_{\alpha,j}$	Cell Galileo number of the α phase, $gd_P^3\varepsilon_j^3/[\mu_\alpha^2(1-\varepsilon_j)^3]$
N	total number of cells (= 256 in this study)
$\Delta P/\Delta Z$	pressure drop per unit cell length, N/m^3
$Re_{\alpha,j}$	cell Reynolds number of the α phase, $V_\alpha d_P/(\mu_\alpha(1-\varepsilon_j))$
r	number of cells in each row (X direction)
s_i	cell face area at a given coordinate direction i, m^2
$s_{w,j}$	liquid saturation in cell j ($\varepsilon_{L,j}/\varepsilon_j$)
$V_{j,\alpha}$	superficial velocity of phase α in the jth cell, m/s
$(\mathrm{Vol})_j$	volume of cell j, m^3 ($= \Delta Z \times \Delta X \times \Delta Y$ for rectangular bed)
ΔZ, ΔX, ΔY	size of the cell, m (in this work, $3d_p$ = 0.009 m)

Greek symbols

ε_B	bed porosity (= 0.414)
ε_j	porosity in the jth cell
$\varepsilon_{j,\alpha}$	holdup of phase α in the jth cell
σ	liquid surface tension, N/m (0.072 for water)
$\gamma_i, i = x,z$	the angle of each axis with horizontal plane
$\hat{\Phi}$	the gravitational potential,
μ_α	viscosity of phase α in the bed, $Pa\,s$ (μ_L = 1.0e-3 $Pa\,s$; μ_G = 1.8e-5 $Pa\,s$)
ρ_α	density of phase α in the bed, kg/m^3 (ρ_L = 1000 kg/m^3; ρ_G = 1.2 kg/m^3)
$\psi_{\alpha,j}$	dimensionless pressure-drop for phase α, $[= (\Delta P_\alpha/\Delta L)/\rho_\alpha g + 1]$

References

Ahtchi-Ali, B., & Pederson, H. (1986). Very large lattice model of liquid mixing in trickle beds. *Ind. Engng Chem. Fund.*, *25*, 108.

Chaouki, J, Larachi, F., & Dudukovic, M.P. (1997) Non-invasive monitoring of multiphase flows. Amsterdam: Elsevier Science B. V.

Crine, M, Marchot, P., & L'Homme, G.A. (1979). Mathematical modeling of the liquid trickling flow through a packed bed using the percolation theory. *Comput. Chem. Engng*, *3*, 515.

Fox, R.O. (1987). One the liquid flow distribution in trickle-bed reactors. *Ind. Engng Chem. Res.*, *26*, 2413.

Funk, G.A., Harold, M.P., & Ng, K.M. (1990). A Novel model for reaction in trickle beds with flow maldistribution, *Ind. Engng Chem. Res.*, *29*, 738.

Grosser, K.A., Carbonell, R.G., & Sundaresan, S. (1988). Onset of pulsing in two-phase cocurrent downflow through a packed bed. *A.I.Ch.E. J.*, *34*, 1850.

Herskowitz, M., & Smith, J.M. (1979). Liquid distribution in trickle-bed reactors. *A.I.Ch.E. J.*, *24*, 439.

Holub, R.A. (1990). *Hydrodynamics of trickle bed reactors.* Ph.D. thesis, Washington University in St. Louis, MO, USA.

Holub, R.A., Dudukovic, M.P., & Ramachandran, P. A. (1992). A phenomenological model for pressure drop, liquid holdup, and flow regime transition in gas–liquid trickle flow. *Chem. Engng Sci.*, *47*, 2343–2348.

Holub, R.A., Dudukovic, M.P., & Ramachandran, P.A. (1993). Pressure drop, liquid holdup, and flow regime transition in trickle flow. *A.I.Ch.E. J. 39*, 302–321.

Jaynes, E.T. (1980). *Ann. Rev. Phys. Chem.*, *31*, 579.

Jiang, Y., Khadilkar, M.R., Al-Dahhan, M.H., & Dudukovic, M.P. (1998). Flow modeling with internal nonuniformities. *Chem. Engng Sci.* submitted.

Kantzas, A. (1994). Computation of holdups in fluidized and trickle beds by computer-assisted tomography. *A.I.Ch.E. J.*, *40*, 1254.

Kashiwa, B.A., Padial, N.T., Rauenzahn, R.M., & W.B. VanderHeyden (1994). A cell centered ICE method for multiphase flow simulations. *ASME Symposium on Numerical Methods for Multiphase Flows*, Lake Tahoe, Nevada.

Kumar, S. (1994). *CREL Annual Meeting*, St. Louis, MO, USA.

Levec, J., Saez, A.E., & Carbonell, R.G., (1986). The hydrodynamics of trickling flow in packed beds. Part II: Experiemental observations, *A.I.Ch.E. J. 32*, 369.

Leverett, M.C. (1941). Capillary behavior in porous solid, *Trans. AIME*, *142*, 159.

Lutran, P.G., Ng, K.M., & Delikat, E.P. (1991). Liquid distribution in trickle beds. An experimental study using computer-assisted tomography, *Ind. Engng Chem. Res.*, *30*, 1270.

Melli, T.R., & Scriven, L.E. (1991). Theory of two-phase cocurrent downflow in networks of passages, *Ind. Engng Chem. Res.*, *30*, 951.

Ravindra, P.V., Rao, D.P. Rao, M.S. (1997). Liquid flow texture in trickle-bed reactors: an experimental study, *Ind. Engng Chem. Res.*, *36*, 5133.

Saez, A.E., & Carbonell, R.G. (1985). Hydrodynamic parameters for gas-liquid cocurrent flow in packed beds, *A.I.Ch.E. J.*, *31*, 52.

Stanek, V., Hanika, J., Hlavacek, V. & Tranka, O. (1981). The effect of liquid Flow distribution on the behavior of a trickle bed reactor, *Chem. Engng Sci. 36*, 1045.

Stanek, V. (1994) *Fixed Bed Operations*: *flow distribution and efficiency*, Ellis Horwood Series in Chemical Engineering.

Toye, D., Marchot, P., Crine, M., & L'Homme, G. (1994). The use of large scale computer assisted tomography for the study of hydrodynamics in trickling filters, *Chem. Engng Sci. 49*, 5271.

Vortmeyer, D., & Winter, R.P., (1984), Improvements in reactor analysis incorporating porosity and velocity profiles, *Ger. Chem. Engng*, *7*, 19.

Zimmerman, S.P., & Ng, K.M. (1986). Liquid distribution in trickling flow trickle bed reactors, *Chem. Engng Sci.*, *41*, 861.